Int. J. Electrochem. Sci., 12 **(2017)** 2583 – 2592, doi: 10.20964/2017.03.73

International Journal of ELECTROCHEMICAL SCIENCE
www.electrochemsci.org

Short Communication

Capacitance of MnO_2 Micro-Flowers Decorated CNFs in Alkaline Electrolyte and Its Bi-Functional Electrocatalytic Activity toward Hydrazine Oxidation

Seong-Min Ji[1], *Zafar Khan Ghouri*[2], *Khaled Elsaid*[3],*Yo Han Ko*[4], *Saeed Al-Meer*[2],*M.I.Ahmad*[2] *Dong Ick Son*[4], *Hak Yong Kim*[1,*]

[1] Department of Bin Fusion Technology, Chonbuk National University, Jeonju 561-756, Republic of Korea
[2] Central Laboratory Unit, Qatar University, P. O. Box: 2713, Doha, Qatar
[3] Chemical Engineering Program, Texas A&M University at Qatar, P.O. 23874, Doha, Qatar
[4] Institute of Advanced Composite Materials, Korea Institute of Science and Technology (KIST), Jeonbuk 565-905, Republic of Korea
[*]E-mail: khy@jbnu.ac.kr

Received: 9 December 2016 / *Accepted:* 28 January 2017 / *Published:* 12 February 2017

Well-dispersed MnO_2 micro-flowers were grown directly on carbon nanofibers via a simple hydrothermal technique without any template. Structure and morphology were characterized by X-ray diffraction (XRD) and field-emission scanning electron microscopy (FESEM) equipped with rapid energy dispersive analysis X-ray (EDX). The appealed characterization techniques specified that the obtained material is carbon nanofibers decorated by MnO_2 micro-flowers. Super capacitive performance of the MnO_2 micro-flowers decorated CNFs as active electrode material was evaluated by cyclic voltammetry (CV) in alkaline medium and yield a reasonable specific capacitance of 120 Fg^{-1} at 5 mV s^{-1}. As an electrocatalyst for hydrazine oxidation, the MnO_2 micro-flowers decorated CNFs showed high current density. The impressive bi-functional electrochemical activity of MnO_2 micro-flowers decorated CNFs is mainly attributed to its unique architectural structure.

Keywords: Supercapacitors; Bi-functional; Carbon nanofibers; MnO_2, Hydrazine; Direct liquid fuel cells.

1. INTRODUCTION

Depletion of global fossil oil resources and environmental concerns has been the theme topics of the world economic and political circles over the past decades. It has been reported that a significant portion of the total energy supply comes from fossil fuels, such as coal, oil, and natural gas, causing a dramatic buildup of greenhouse gasses GHGs in the atmosphere. In order to fulfill the growing

demand for clean and high-efficient energy, an alternative energy resource that independent of fossil fuels must be developed [1-5].

Supercapacitors (also known as electrochemical capacitors) and direct liquid fuel cells are the most promising devices in the field of energy conversion and storage [6, 7]. Comparing with other types of direct liquid fuel cells, direct hydrazine fuel cell (DHFC) achieves a zero pollution emission; only nitrogen and water are produced during the oxidation process. Moreover, there is no catalyst poisoning in direct hydrazine fuel cells. Similarly, supercapacitors are likely to show equal importance to batteries and fuel cells for future energy storage system due to their high power characteristics compared to batteries, high energy density compared to conventional capacitors, long cycling life and short charging time [8, 9].

The energy storage/conversion processes for supercapacitors be defined in two ways and commonly classified as electrochemical double layer capacitors (EDLCs) and pseudocapacitors [10, 11]. In EDLCs energy is stored electrostatically while pseudocapacitors utilize fast and reversible Faradaic reactions between the electrolyte and electro-active materials [1]. Electrode /catalyst materials are the key elements to determine device performance; thus they have received great attention in recent years [6, 12-14].

In particular, cheap transition metal oxide based catalysts are desirable for both supercapacitors and fuel cells; because they are electrochemically more active. Therefore, recent work has been focused on the synthesis and use of non-precious transition metal oxides. Among the auspicious substitute electrode material, MnO_2 has been of specific attention for the past decade because of its abundance, low cost, high catalytic activity and non–toxicity, but their poor electrical conductivity and low structural stability constrain their practical application [15].

To address these problems, a template-free design of 3D open architecture process has been developed [16-18]. MnO_2 in the shape of micro-flower have been considered as one of the optimal nanostructures because of the fully exposed structure/high surface area which can facilitate the transportation of electrons and cations. But, the synthesis of flower-like architecture still faces a challenge owing to the fast and complex growing process.

Therefore, it is desirable to develop facile, environment-friendly, low-cost, and template-free synthetic methods for the fabrication of MnO_2 micro-flowers with rich and proper porosity. Herein, we present a facile self-assembled synthesis of MnO_2 micro-flowers decorated carbon nanofibers, which have extensively identified in terms of morphology and crystallinity. Moreover, the electrochemical properties of the material have been investigated for application as supercapacitor and electrocatalyst for hydrazine oxidation in an alkaline medium.

2. EXPERIMENTAL

2.1 Procedure

2.1.1. Materials

Manganese (II) nitrate tetrahydrate (≥97%) (Junsei Chemical Co. Japan), Poly (Vinyl alcohol) (PVA) with a molecular weight 65000 g/mol (Sigma-Aldrich Corporation, St. Louis MO USA), and distilled water as a solvent.

2.1.2. Preparation of MnO_2 micro-flowers decorated CNFs

The procedures used for carbon nanofibers synthesis in this study have followed those previously developed and described by the group [2,3]. In a typical synthesis of MnO_2 micro-flowers decorated CNFs, 0.01 mol/L manganese nitrate was added to 120 mL deionized water under vigorous stirring. 0.05mol/L urea, $CO(NH_2)_2$ was then added to the solution, and the solution was transferred into a 150 mL Teflon-lined stainless steel autoclave. A piece of CNFs mat was subsequently soaked in the solution, followed by autoclave heating in an oven at 90 ℃ for 10h. The synthesized sample was then taken out, cleaned several times with DI water and ethanol, dried at 80 ℃ for about an hour and annealed at 350 ℃ in air for 2 hours.

2.2. Electrode Preparation and electrochemical measurement

Based on our previous work [2,3], working electrode was prepared with 2mg of the active electrocatalyst, 20 μL of Nafion solution, and 400 μL of isopropanol while the electrochemical measurements were carried out in the conventional three-electrode electrochemical cell (VersaSTAT 4, USA) at room temperature in 1M KOH solution.

2.3. Sample characterization

The morphology of the MnO_2 micro-flowers decorated carbon nanofibers was observed by field-emission scanning electron microscopy (FESEM, Hitachi S-7400, japan), coupled with rapid energy dispersive analysis of X-Ray (EDX) system. The phase and crystallinity of the composite were characterized by X-ray diffractometer (XRD, Rigaku, Japan) with Cu-Kα (λ=1.54056 Å) radiation operating at 45kV and 100mA over a range of 2θ angle from 10^o to 80^o, scanning at a rate of 4^o/ min.

3. RESULT AND DISCUSSION

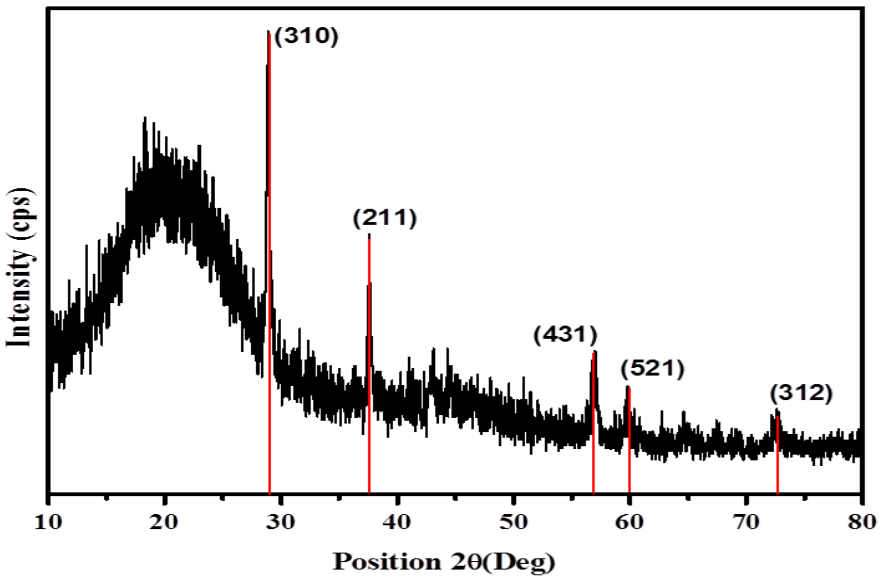

Figure 1. XRD spectra for the obtained electrospun MnO_2 micro-flowers decorated CNFs after annealing at 350℃ in air for 2hrs.

The phase composition and phase structure of as-obtained nanostructure were examined by X-ray powder diffraction (XRD). Fig. 1 displays the XRD spectrogram of MnO_2 micro-flowers decorated CNFs. Comparing XRD spectrogram of the synthesized materials with the standard diffraction spectra, the synthesized product is crystalline MnO_2.

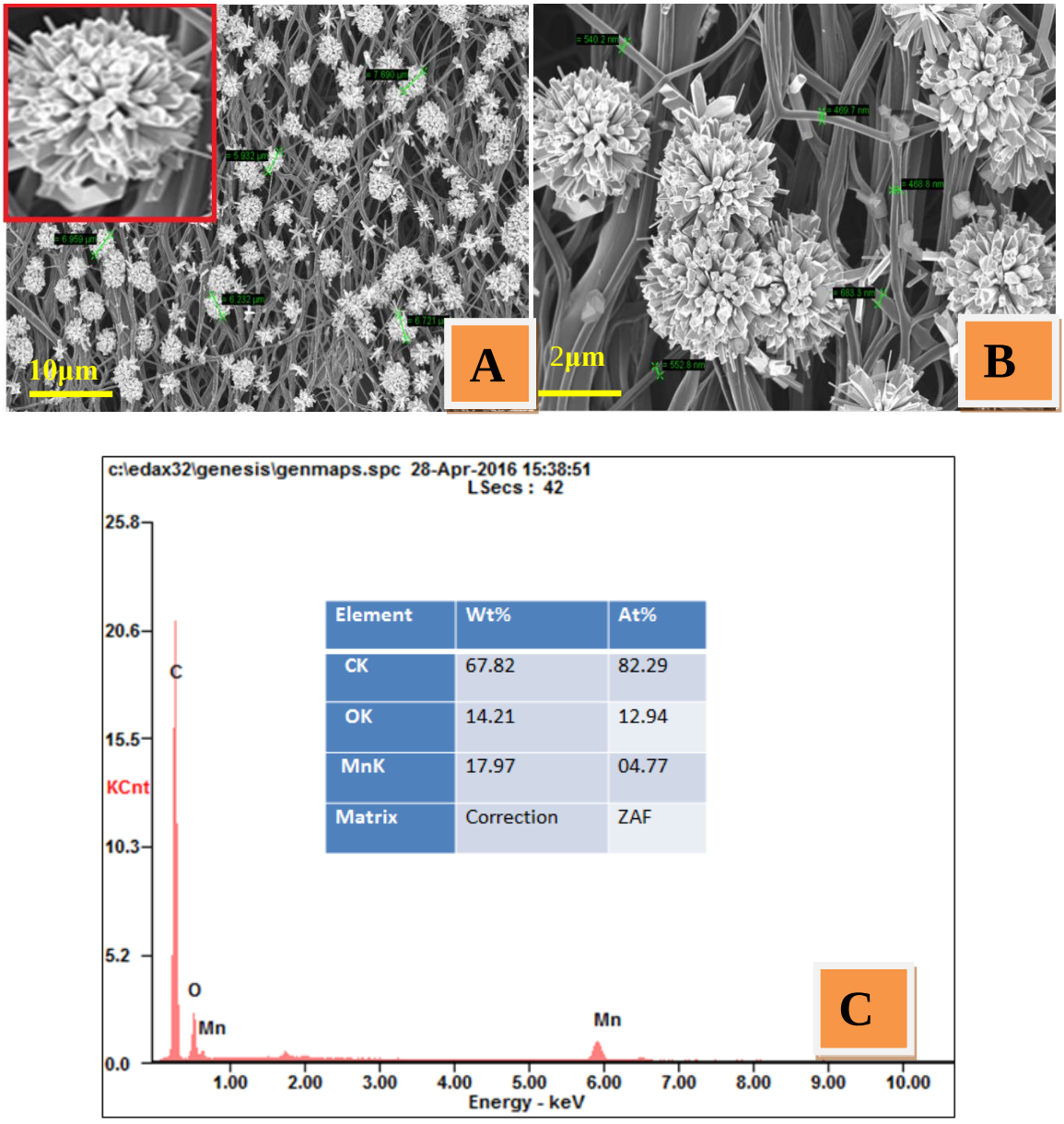

Figure 2. FESEM image of electrospun MnO_2 micro-flowers decorated CNFs (a and b) and EDX spectrum (c) of MnO_2 micro-flowers decorated CNFs after annealed at 350 ℃ in air for 2 hours.

As shown in the obtained XRD pattern, the diffraction peaks at 2θ values of 28.84°, 37.52°, 56.92°, 60.27° and 72.71° indexed as the (310), (211), (431), (521) and (312) crystal planes, respectively indicate formation of MnO_2; the most prominent peak being at 28.84°. This peak can be

correlated to (310) *hkl* indices of pure tetragonal structure [space group: I4/m (87)] according to the JCPDS no.: 00-044-0141 with lattice constants $a=b=9.7847$ Å, $c=2.8630$ Å, $\alpha=\beta=\gamma=90$, suggesting MnO_2 structure mainly grows along the (310) face. The main challenge in developing MnO_2 micro-flowers decorated carbon nanofibers is to incorporate MnO2 micro-flowers attach onto carbon nanofibers uniformly and this attachment is mainly dependent on the synthesis route. In order to crop MnO_2 outgrown on the carbon nanofibers, the nanofibers produced after calcination was allowed to go through a hydrothermal treatment as mentioned in the experimental section.

Fig. 2 represents FESEM images for the product obtained by the hydrothermal treatment. As revealed, the uniform micro-flowers with an average size of about 75 μm outgrown on the surface of nanofibers due to hydrothermal treatment, as shown in Fig. 2.A. At a higher magnification (inset of Fig. 2.A), these micro-flowers show hierarchical structures consisting of nanorods with a diameter of about 15~20 nm and a length of about 1 μm. It is also noticed that the micro-flowers are evenly distributed in the network of carbon nanofibers. The diameter of the carbon nanofibers varies from 400 to 700 nm as shown in Fig. 2.B. From the EDX spectra, as shown in Fig. 2.C, the presence of Manganese (Mn), oxygen (O), and carbon (C) have been detected; with the atomic and weight percentage of manganese, carbon, and oxygen are summarized in the inset in Fig. 2.C.

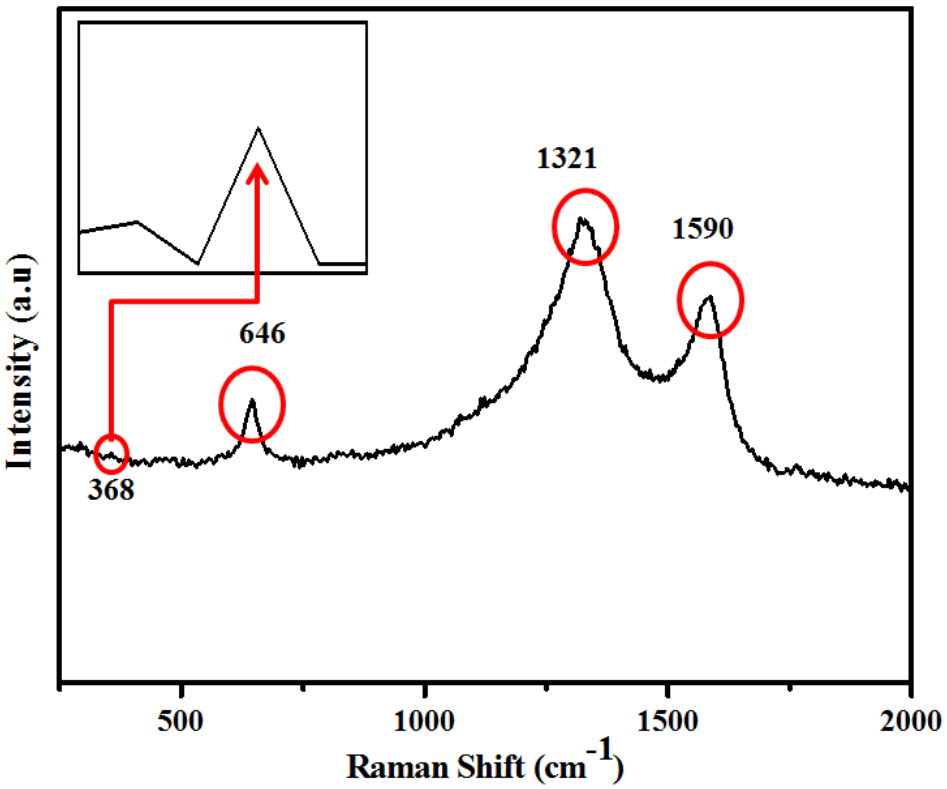

Figure 3. Raman spectra for the obtained electrospun MnO_2 micro-flowers decorated CNFs after annealed at 350 ℃ in air for 2 hours.

Raman spectroscopy was executed as well to examine the local structure of MnO_2 micro-flowers decorated CNFs. As shown in Fig. 3, two broad overlapping peaks centered on 1321 and 1590 cm^{-1} that correspond to the disordered (D band) and graphite (G band), arising from the

disordered structure of carbon [19]. Concerning MnO_2, the Raman peaks observed at 368 (marked by red circles & arrow along with high magnification), and 646 cm^{-1} demonstrate MnO_2 microstructures.

An electrochemical analysis of MnO_2 micro-flowers decorated CNFs performance was carried out using cyclic voltammetry CV. The specific capacitance of the composite can be calculated with CV results according to the following equation [20]:

$$C_{sp} = \frac{1}{2m.\upsilon.\Delta V}\int I(V)dV \qquad (1)$$

Where, C_{sp} is the specific capacitance, m is the mass of the grafted composite, *v is* the potential scan rate, ΔV is the sweep potential window, and I (V) is the voltammetric current on CV curves. Fig. 4 shows the rate-dependent cyclic voltammetry (CV) curves of MnO_2 micro-flowers decorated CNFs at various scan rates (5,10, 25, 50, and 75 mVs^{-1}) between -0.2 V and 1.0 V (vs. Ag/AgCl) in 1 M KOH electrolyte. The CV curves were fairly rectangular in shape, which is a typical capacitive behavior of carbon materials [21]. In addition, the current densities increase along with increasing scan rates, suggesting good rate performance [22].

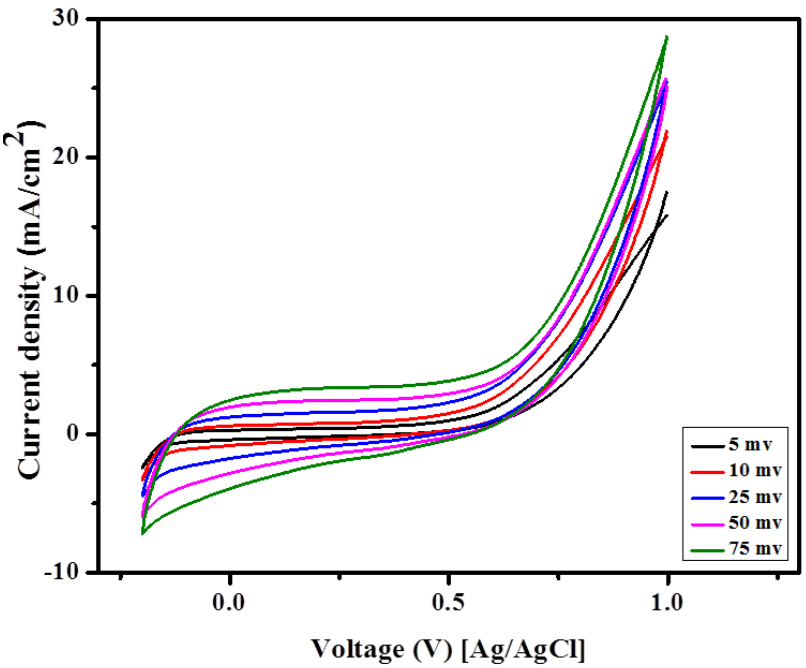

Figure 4. Cyclic voltammograms of the electrospun MnO_2 micro-flowers decorated CNFs in 1 M KOH solution at different scan rates.

The specific capacitances of nanostructure at different scan rates are shown in Fig. 5. The specific capacitance decreases with the increase of scan rates from 5 to 75 mVs^{-1}. At low scan rates (5 mVs^{-1}), both active areas, internal and external, of the electrode surfaces could take part in reaction while at high scan rate (75 mVs^{-1}) the diffusion of the electrolyte ions was limited thus only the external surface area of electrode could participate in ion transfer reaction [23]. As shown in Fig. 5 the maximum specific capacitance obtained at a scan rate of 5 mVs^{-1} of was 120 Fg^{-1}.

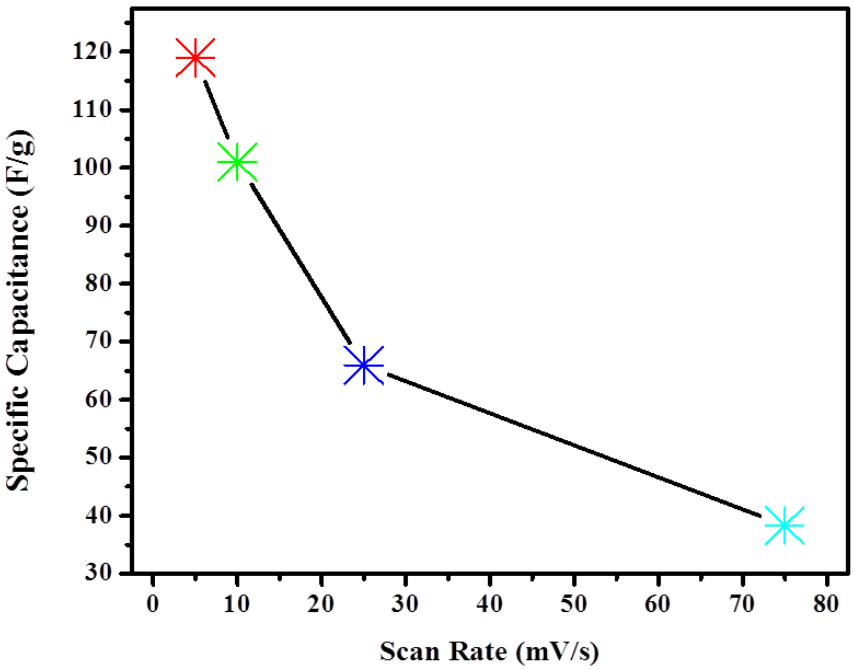

Figure 5. Effect of scan rate on specific capacitance

Comparison of the capacitive performance of MnO_2 micro-flowers @CNFs based electrode and other reported CNFs and the graphene-based electrode was conducted, as shown in table 1. At low scan rate $5mVs^{-1}$, the specific capacitance can reach 120 Fg^{-1} for MnO_2 micro-flowers decorated CNFs, showing a much superior capacitive performance to other reported CNFs and graphene-based electrodes. This result could not only be accredited to the capacitance input of MnO_2 but benefit from the distinctive structure of MnO_2 micro-flowers which could supply more active sites and internal space which electrolyte ions could access easily. Moreover, the support of carbon nanofibers as conducting material could improve conductivity and convenient pathway for ion transfer [26, 27]. Such synergistic effect between carbon nanofibers and manganese oxides micro-flowers had a great effect on improving the capacitive performance of the electrode [28, 29].

Table 1. Comparison of capacitive performance of the Introduced Composite with Some Reported Ones, in KOH as an electrolyte.

Composite/Materials	Capacitance (Fg^{-1})	Reference
Fe/CeO_2@CNFs	57	[24]
MnO_2&Co@Graphene	2.5	[4]
Co/CeO_2@CNFs	9.0	[25]
MnO_2 micro-flowers@CNFs	120	This work

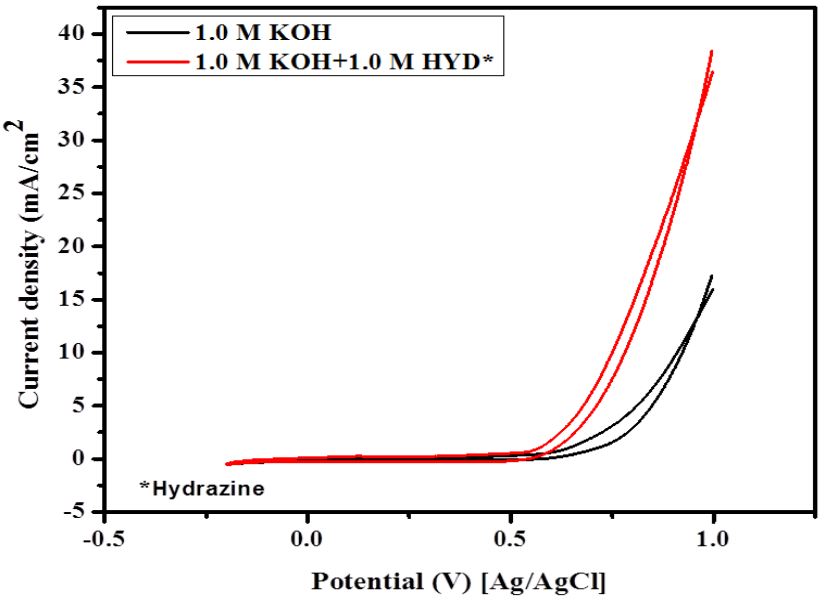

Figure 6. Typical cyclic voltammogram of the electrospun MnO_2 micro-flowers decorated CNFs measured in 1 M KOH and 1 M KOH+0.5 M Hydrazine at 50 mV/s.

The typical catalytic response of MnO_2 micro-flowers decorated CNFs in 1 M KOH with 0.5 M hydrazine is shown in Fig. 6 showing the CV that indicates an excellent electrocatalytic activity of nanostructures by showing effective hydrazine oxidation with high current density in the presence of hydrazine (Red). At the potential of 1 V, the current density of the nanostructure reached 38 $mAcm^{-2}$, which almost double the current density in case of 1 M KOH .

Overall, it is hypothesized that the uniformly embedded electronic conducting network of carbon nanofibers can improve the high-rate capability as well as the specific capacitance of the materials. Moreover, carbon nanofibers network with hierarchical MnO_2 micro-flowers can shorten the diffusion path for charge-carrier ions, whereas the large liquid–solid interface simplifies ion exchange between the electrode and electrolyte [30-33].

4. CONCLUSION

MnO_2 micro-flowers decorated carbons nanofibers hierarchical structure have been prepared by calcination of electrospun nanofibers mats composed of polyvinyl acetate followed by hydrothermal treatment and were demonstrated to be superior bi-functional electrode material for energy conversion and storage devices. MnO_2 micro-flowers decorated carbon nanofibers electrode exhibited a superior capacitance of 120 Fg^{-1} at low scan rate. Interestingly, the MnO_2 micro-flowers decorated carbon nanofibers showed hydrazine electro-oxidation with high current density (38 mA/cm^2). The MnO_2 micro-flowers decorated carbon nanofibers electrode can be a hopeful catalyst for energy conversion and storage devices thanks to its low cost and satisfactory electrocatalytic performance.

ACKNOWLEDGMENTS
This Research was financially supported by National Research Foundation of Korea (NRF) Grant funded by the Korean Government (MSIP) (No. 2014R1A4A1008140).

References

1. Z. K. Ghouri, M. Shaheer Akhtar, A. Zahoor, N. A. M. Barakat, W. Han, M. Park, B. Pant, P. S. Saud, C. H. Lee, and H. Y. Kim, *Journal of Alloys and Compounds*, 642 (2015) 210.
2. Z. K. Ghouri, N. A. M. Barakat, M. Park, B.-S. Kim, and H. Y. Kim, *Ceramics International*, 41 (2015) 6575.
3. Z. K. Ghouri, N. A. M. Barakat, M. Obaid, J. H. Lee, and H. Y. Kim, *Ceramics International*, 41(2015) 2271.
4. Z. K. Ghouri, N. A. Barakat, and H. Y. Kim, *Energy and Environment Focus*, 4 (2015) 34.
5. Z. K. Ghouri, N. A. M. Barakat, and H. Y. Kim, *Scientific Reports*, 5 (2015) 16695.
6. P. Simon and Y. Gogotsi, *Nat Mater*, 7 (2008) 845.
7. R. Liu, K. Ye, Y. Gao, Z. Long, K. Cheng, W. Zhang, G. Wang, and D. Cao, *Materials Science and Engineering: B*, 210 (2016) 51.
8. D. Chen, L. Tang, and J. Li, *Chemical Society Review*, 39 (2010) 3157.
9. M.-y. Zhang, X.-j. Jin, and Q. Zhao, *New Carbon Materials*, 29 (2014) 89.
10. G. Wang, L. Zhang, and J. Zhang, *Chemical Society Reviews*, 41 (2012) 797.
11. Frackowiak, *Physical Chemistry Chemical Physics*, 9 (2007) 1774.
12. A. S. Arico, P. Bruce, B. Scrosati, J.-M. Tarascon, and W. van Schalkwijk, *Nat Mater*, 4 (2005) 366.
13. X. Zhao, B. M. Sanchez, P. J. Dobson, and P. S. Grant, *Nanoscale*, 3 (2011) 839.
14. M. Zhi, C. Xiang, J. Li, M. Li, and N. Wu, *Nanoscale*, 5 (2013) 72.
15. Z. K. Ghouri, A. Zahoor, N. A. M. Barakat, M. S. Alsoufi, T. M. Bawazeer, A. F. Mohamed, and H. Y. Kim, *Superlattices and Microstructures*, 90 (2016) 184.
16. W. Yang, Z. Gao, J. Wang, B. Wang, Q. Liu, Z. Li, T. Mann, P. Yang, M. Zhang, and L. Liu, *Electrochimica Acta*, 69 (2012) 112.
17. M. Xu, L. Kong, W. Zhou, and H. Li, *The Journal of Physical Chemistry* C, 111 (2007) 19141.
18. A. Yuan, X. Wang, Y. Wang, and J. Hu, *Electrochimica Acta*, 54 (2009) 1021.
19. J. Liwen and Z. Xiangwu, *Nanotechnology*, 20 (2009) 155705.
20. Z. K. Ghouri, N. A. Barakat, A.-M. Alam, M. S. Alsoufi, T. M. Bawazeer, A. F. Mohamed, and H. Y. Kim, *Electrochimica Acta*, 184 (2015) 193.
21. I.-T. Kim, N. Kouda, N. Yoshimoto, and M. Morita, *Journal of Power Sources*, 298 (2015) 123.
22. P. Lv, Y. Y. Feng, Y. Li, and W. Feng, *Journal of Power Sources*, 220 (2012) 160.
23. J.-G. Wang, Y. Yang, Z.-H. Huang, and F. Kang, *Journal of Power Sources*, 224 (2013) 86.
24. Z. K. Ghouri, N. Barakat, A.-M. Alam, M. Park, T. H. Han, and H. Y. Kim, *Int. J. Electrochem. Sci.*, 10 (2015) 2064.
25. J. Kim, Z. K. Ghouri, R. Z. Khan, T. An, M. Park, and H.-Y. Kim, *Carbon letters*, 16 (2015) 270.
26. W. Wei, X. Cui, W. Chen, and D. G. Ivey, *Chemical Society Reviews*, 40 (2011) 1697.
27. M. Liu, L. Gan, W. Xiong, F. Zhao, X. Fan, D. Zhu, Z. Xu, Z. Hao, and L. Chen, *Energy & Fuels*, 27 (2013) 1168.
28. C.-C. Lai and C.-T. Lo, *Electrochimica Acta*, 183 (2015) 85.
29. A. Gambou-Bosca and D. Bélanger, *Journal of Power Sources*, 326 (2016) 595.
30. D. Eder, *Chemical reviews*, 110 (2010) 1348.

31. C.-T. Hsieh, D.-Y. Tzou, W.-Y. Lee, and J.-P. Hsu, *Journal of Alloys and Compounds,* 660 (2016) 99.
32. A. Gambou-Bosca and D. Bélanger, *Electrochimica Acta*, 201 (2016) 20.
33. A. Zolfaghari, H. R. Naderi, and H. R. Mortaheb, *Journal of Electroanalytical Chemistry,* 697 (2013) 60.

© 2017 The Authors. Published by ESG (www.electrochemsci.org). This article is an open access article distributed under the terms and conditions of the Creative Commons Attribution license (http://creativecommons.org/licenses/by/4.0/).